JOURNAL OF GUIDANCE, CONTROL, AND DYNAMICS
Vol. 32, No. 5, September–October 2009

Engineering Notes

Computational Bifurcation Analysis of Multiparameter Dynamical Systems

N. Ananthkrishnan* and Nitin K. Gupta†
IDeA Research & Development (P), Ltd., Pune 411001, India
and
Nandan K. Sinha‡
Indian Institute of Technology Madras, Chennai 600036, India

DOI: 10.2514/1.44173

I. Introduction

DYNAMICAL systems in many areas of science and engineering are modeled as a set of nonlinear ordinary differential equations of the following form:

$$\dot{x} = f(x, \lambda) \tag{1}$$

where x is an n-dimensional vector of states, λ are m independent parameters, and f is an n-dimensional vector of nonlinear functions. These systems show a host of interesting nonlinear dynamic behavior, such as multiple attractors, limit cycles, jump phenomena, hysteresis, frequency locking, and chaos [1]. Nonlinear behaviors such as these are best understood in terms of bifurcations of the dynamical system, which is a record of all critical points in the $(n + m)$-dimensional state-parameter space in which equilibrium and periodic solutions of Eq. (1) are either created, destroyed, or undergo a change in their stability. Results from bifurcation theory can then be used to describe the possible dynamic behavior of the system as it encounters any of these bifurcation points. Bifurcation methods have been widely used, for instance, to study nonlinear phenomena in aircraft flight dynamics [2].

A bifurcation analysis must begin by computing all equilibrium and periodic solutions of that system along with information about the stability of these solutions. The equilibrium solutions form (hyper) surfaces in the state-parameter space, for example, a system with one state variable and two parameters would have a two-dimensional surface of equilibrium solutions in a $(1 + 2)$-dimensional state-parameter space. Unfortunately, for higher-dimensional systems with multiple parameters, both computing and visualizing the equilibrium surfaces is exceedingly difficult [3]. Instead, the standard procedure until recently [4] has been to compute what is called a bifurcation diagram, that is, curves of equilibrium solutions as one of the parameters is varied while all the other parameters are held fixed. This procedure may be repeated by sequentially selecting another parameter to be the variable, thus generating an entire family of bifurcation diagrams.

Traditionally, therefore, bifurcation analysis of a multiparameter dynamical system involves solving a series of one-parameter problems of the following form:

$$\dot{x} = f(x, \lambda_1, \lambda_j = k_j), \qquad j = 2, \ldots, m \tag{2}$$

or

$$\dot{x} = f(x, \lambda_1, \lambda_j = k_j\lambda_1), \qquad j = 2, \ldots, m \tag{3}$$

where λ_1 is the principal continuation parameter, and the k_j constrain the values of the other parameters λ_j. To give a concrete example, consider a five-state, three-parameter system in the form of Eq. (1) for the dynamics of an airplane performing a rapid rolling maneuver. The equations of motion for the airplane dynamics (see the Appendix) and the associated data are the same as in [5]. The five states, x_1–x_5, are, sequentially, the roll, pitch, and yaw rates, the angle of attack, and the sideslip angle; the three parameters, λ_1–λ_3, are, sequentially, the aileron deflection, rudder deflection, and elevator deflection. This system is known from a previous study [6] to exhibit two transcritical bifurcation branches, that is, a one-dimensional locus of transcritical points in an eight-dimensional state-parameter space. With λ_2 and λ_3 constrained as $\lambda_2 = k_2\lambda_1$ and $\lambda_3 = k_3$, a bifurcation analysis is carried out with aileron deflection λ_1 as the principal continuation parameter. The bifurcation diagram for roll rate x_1 (other states are qualitatively similar) for five different values of k_2 is shown in Fig. 1.§

Cases 1 and 2 show no bifurcation point, and cases 4 and 5 show two turning points each, whereas the intermediate, case 3, shows a single transcritical bifurcation. For this computation, the solutions for cases 1 and 2 and 4 and 5 were first obtained, and the presence of a transcritical point was inferred from the change in the qualitative dynamics of the system between cases 2 and 4. Then, starting with one of the turning points (case 4 or 5), a two-parameter continuation of the turning points was carried out to trace the locus of turning points in the λ_1–λ_2 space (or, equivalently, in the λ_1–k_2 space). A turning point of this locus signifies the presence of a transcritical bifurcation and gives the value of k_2, corresponding to case 3 in Fig. 1. Another computation using precisely this value of k_2 was then required to obtain the bifurcation diagram with the transcritical bifurcation point. Care is required because a small perturbation in the value of k_2 is often enough to miss the transcritical point, giving a solution of the type of either case 2 or 4. However, the solution is still incomplete and further computations with a variation of parameter λ_3 are required to locate the second branch of transcritical bifurcation points known to exist for this dynamical system.

In contrast, the new approach proposed in this Note can, in principle, provide the complete bifurcation diagram of a multiparameter system with a single computation, unlike the sequential one-parameter approach in [4]; it is also computationally efficient, unlike the surface tracking technique in [3].

II. New Approach

The key to our approach is to recognize that multiple (in principle, all) bifurcations in the state-parameter space may be captured by a single computation solving

$$\dot{x} = f(x, \lambda_1, \lambda_j = k_j(\lambda_1)), \qquad j = 2, \ldots, m \tag{4}$$

For instance, in a $(1 + 2)$-dimensional state-parameter space, the constraints k_j in Eqs. (2) and (3) are planes and, hence, may not, in general, be expected to intersect multiple, or even one, bifurcation point in space. In contrast, the constraints k_j in Eq. (4) are arbitrary surfaces and could be made to pass through as many bifurcation points as desired.

Received 6 March 2009; accepted for publication 6 July 2009.

*Director. Associate Fellow AIAA.
†CEO.
‡Department of Aerospace Engineering.

§The AUTO2000 software (http://indy.cs.concordia.ca/auto/) has been used for all computations reported here [retrieved 13 July 2009].

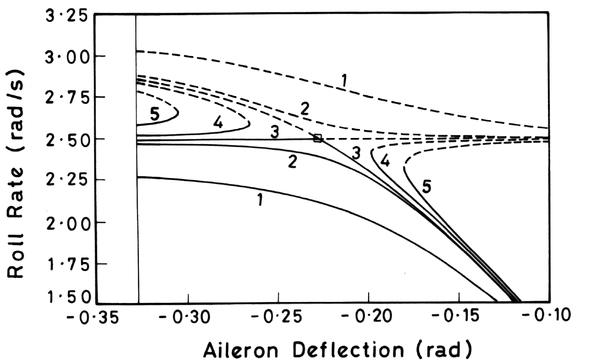

Fig. 1 Bifurcation diagram from the traditional approach carried out for five different values of k_2, labeled 1–5 (full line: stable; dashed line: unstable; open square: transcritical bifurcation).

More rigorously, consider a $(1 + 2)$-dimensional system in the form of Eq. (1) for which the equilibrium points lie on a surface given by $f(x, \lambda_1, \lambda_2) = 0$. Letting $\lambda_2(s) = k_2(\lambda_1(s))$, where s is the arc length, the following condition can be obtained:

$$\left(\frac{\partial f}{\partial x}\right)_* = \frac{[(\frac{\partial f}{\partial \lambda_1})_* + (\frac{\partial f}{\partial \lambda_2})_* k_2'(\lambda_1)]\frac{d\lambda_1}{ds}}{(\frac{dx}{ds})} \qquad (5)$$

where $*$ indicates that the quantity in parenthesis is evaluated at the equilibrium point, and prime denotes the derivative of k_2 with respect to λ_1. For a one-dimensional system, the quantity on the left-hand side of Eq. (5) is nothing but the eigenvalue at a given equilibrium point. It follows that, at an equilibrium point with a zero eigenvalue, either $d\lambda_1/ds = 0$, that is, it is a turning point, or the bracketed term on the right-hand side is 0, that is, it is a (transcritical or pitchfork) bifurcation point. In Eq. (2), $k_2'(\lambda_1) = 0$, and an additional condition, $(\partial f/\partial \lambda_1)_* = 0$, is required for the equilibrium point to be a bifurcation point. In Eq. (3), $k_2'(\lambda_1) = k_2$, and a bifurcation point is obtained for particular values of k_2 for which the bracketed term on the right-hand side becomes 0. Clearly, using Eqs. (2) and (3), bifurcation points are encountered only under special circumstances. On the other hand, with Eq. (4), $k_2'(\lambda_1)$ could be chosen to make the right-hand bracket equal 0 at as many bifurcation points as desired, making it possible to capture multiple bifurcations with a single computation.

The issue, then, is how to prescribe the constraint functions k_j. One method for doing so is described here; however, it does not guarantee that *all* bifurcation points will be captured. The question remains open and is a matter for future research.

A. Prescribing the Constraint Functions k_j

Construct an $(m - 1)$-dimensional constraint function on the state variables x of the form $y = g(x) = 0$. The functions k_j are then *computed as part of the solution* by solving the following set of $(n + m - 1)$ nonlinear algebraic equations in the $(n + m - 1)$ unknowns x, k_j, and the single parameter λ_1:

$$f(x, \lambda_1, k_j(\lambda_1)) = 0, \qquad j = 2, \ldots, m, \quad \text{and} \quad g_k(x) = 0 \qquad k = 2, \ldots, m \qquad (6)$$

The constraints $g(x) = 0$ could be selected based on the physics of the problem at hand. Consequently, the solved functions $k_j(\lambda_1)$ happen to be the required variation of the parameters λ_2 to λ_m to constrain the equilibrium points of the system to the region of state space defined by the functions $g_k(x) = 0$, $k = 2, \ldots, m$.

A test for the well posedness of the functions $g_k(x)$ is available from the machinery of the Lie derivative, commonly used in nonlinear control theory [7].

B. Application to Example Problem

The procedure is now demonstrated on the aircraft roll dynamics problem discussed earlier. The algorithm employed here is the same as that used in our earlier work on extended bifurcation analysis [8].

The two constraint equations are taken to be of the following form:

$$y_2 = g_2(x) = x_5 = 0, \qquad y_3 = g_3(x) = x_2 + 0.18 = 0 \qquad (7)$$

for the purpose of this illustration. The numerical values chosen here are not special; they are taken from the steady-state values attained after a representative time simulation. To test the well posedness, each constraint function $y_k = g_k(x) = 0$ is differentiated with respect to time:

$$\dot{y}_k = \frac{\partial g_k}{\partial x_i}\dot{x}_i = \frac{\partial g_k}{\partial x_i} f_i(x, \lambda_1, k_j(\lambda_1)) = L_f(g_k) = 0 \qquad (8)$$

where the repeated index implies summation, and $L_f(g_k)$ is the Lie derivative. If necessary, higher Lie derivatives, such as $L_f^2(g_k)$ and so on, are taken until a particular k_j appears in the expression for the Lie derivative. For the present example, it can be verified that the parameter functions k_2 and k_3, respectively, appear in the constraint equations in Eq. (7) on taking the second derivative of y_2 and first derivative of y_3. The seven-dimensional system obtained from the equilibrium equations in the Appendix (by setting the left-hand side to 0) and the constraint equations in Eq. (7) is therefore well posed. Its solution yields the parameter functions, $k_2(\lambda_1)$ and $k_3(\lambda_1)$, viz., rudder and elevator deflections; these are plotted in Fig. 2.

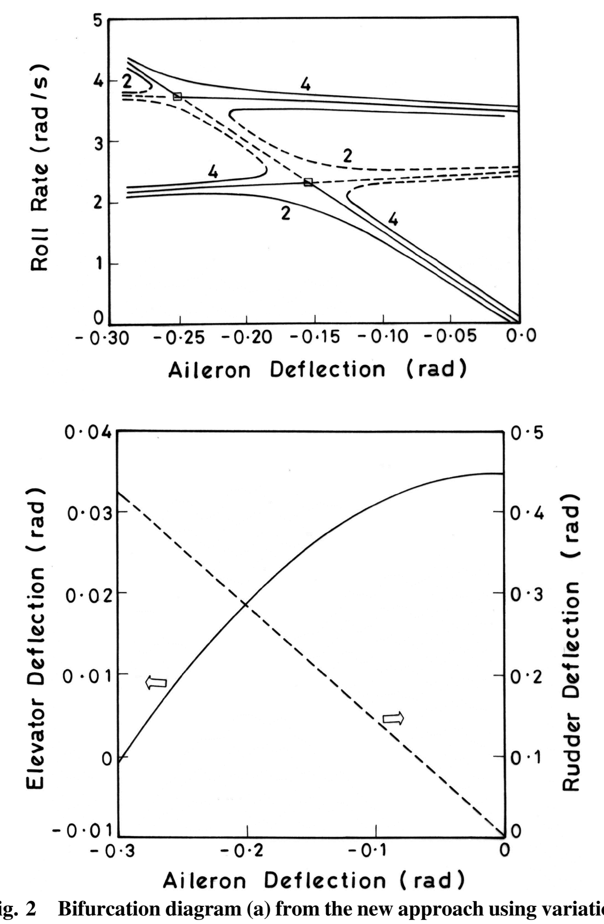

Fig. 2 Bifurcation diagram (a) from the new approach using variation of rudder and elevator deflection parameters (b) required to satisfy the state variable constraints in (7) (full line: stable; dashed line: unstable; open square: transcritical bifurcation). Cases 2 and 4 correspond qualitatively to those in Fig. 1. Arrows in Fig. 2b relate each graph to the labels on the vertical axis.

C. Multiparameter Bifurcation Analysis

Bifurcation analysis of the three-parameter dynamical system in the Appendix is now carried out in the manner of Eq. (4), with λ_2 and λ_3 varying as per the functions $k_2(\lambda_1)$ and $k_3(\lambda_1)$ computed earlier, and λ_1 being the principal continuation parameter. Note that all parameters are varied simultaneously; hence, this is a true multiparameter analysis. A single computation gives the complete bifurcation diagram; for example, roll rate x_1 (other states are qualitatively similar) showing both the transcritical bifurcation points is plotted in Fig. 2. For comparison, Fig. 2 also shows solutions qualitatively similar to those labeled 2 and 4 in Fig. 1; these are obtained by slightly perturbing the parameter functions $k_2(\lambda_1)$ and $k_3(\lambda_1)$ from their computed value. Figure 2 completely captures the qualitative behavior of the dynamical system in question.

III. Conclusions

In this Note, we have presented a radically new approach to computing bifurcation diagrams for dynamical systems with multiple parameters. Using our approach, it is possible to capture multiple bifurcation points with a single computation, and this is illustrated with an example of a five-state, three-parameter dynamical system from aircraft flight dynamics. There is scope for devising better and more rigorous algorithms to arrive at the parameter constraint function, which forms the underpinning of our approach.

Appendix: Equations of Motion: Airplane Roll Dynamics

$$\dot{x}_1 = l_\beta x_5 + l_p x_1 + l_r x_3 - x_2 x_3 (I_z - I_y)/I_x + l_{\delta a}\lambda_1 + l_{\delta r}\lambda_2 \quad \text{(A1)}$$

$$\dot{x}_2 = m_\alpha x_4 + m_{\dot{\alpha}} \dot{x}_4 + m_q x_2 + x_1 x_3 (I_z - I_x)/I_y + m_{\delta e}\lambda_3 \quad \text{(A2)}$$

$$\dot{x}_3 = n_\beta x_5 + n_p x_1 + n_r x_3 - x_1 x_2 (I_y - I_x)/I_z + n_{\delta a}\lambda_1 + n_{\delta r}\lambda_2 \quad \text{(A3)}$$

$$\dot{x}_4 = x_2 - x_1 x_5 + z_\alpha x_4 \quad \text{(A4)}$$

$$\dot{x}_5 = x_1 x_4 - x_3 + y_\beta x_5 \quad \text{(A5)}$$

References

[1] Strogatz, S. H., *Nonlinear Dynamics and Chaos*, Addison–Wesley, Reading, MA, 1994, pp. 1–11.

[2] Paranjape, A. A., Sinha, N. K., and Ananthkrishnan, N., "Use of Bifurcation and Continuation Methods for Aircraft Trim and Stability Analysis—A State-of-the-Art," *Journal of Aerospace Sciences and Technologies*, Vol. 60, No. 2, 2008, pp. 85–100.

[3] Henderson, M. E., "Multiple Parameter Continuation: Computing Implicitly Defined *k*-Manifolds," *International Journal of Bifurcation and Chaos in Applied Sciences and Engineering*, Vol. 12, No. 3, 2002, pp. 451–476.
doi:10.1142/S0218127402004498

[4] Chang, S.-L., Chien, C.-S., and Jeng, B.-W., "Tracing the Solution Surface with Folds of a Two-Parameter System," *International Journal of Bifurcation and Chaos in Applied Sciences and Engineering*, Vol. 15, No. 8, 2005, pp. 2689–2700.
doi:10.1142/S0218127405013630

[5] Sinha, N. K., and Ananthkrishnan, N., "Maximum Steady Roll Rate in Zero-Sideslip Roll Maneuvers of Aircraft," *Journal of Aircraft*, Vol. 39, No. 5, 2002, pp. 897–899.
doi:10.2514/2.3014

[6] Ananthkrishnan, N., and Sudhakar, K., "Prevention of Jump in Inertia-Coupled Roll Maneuvers of Aircraft," *Journal of Aircraft*, Vol. 31, No. 4, 1994, pp. 981–983.
doi:10.2514/3.46591

[7] Slotine, J.-J. E., and Li, W., *Applied Nonlinear Control*, Prentice–Hall, Englewood Cliffs, NJ, 1991, pp. 229–230.

[8] Ananthkrishnan, N., and Sinha, N. K., "Level Flight Trim and Stability Analysis Using Extended Bifurcation and Continuation Procedure," *Journal of Guidance, Control, and Dynamics*, Vol. 24, No. 6, 2001, pp. 1225–1228.
doi:10.2514/2.4839